



Positron annihilation lifetime spectroscopy study of roller burnished magnesium alloy

Radosław Zaleski,
Kazimierz Zaleski,
Marek Gorgol

Abstract. The effect of roller burnishing on Vickers' hardness and positron lifetimes in the AZ91HP magnesium alloy was studied. The microhardness increases with an increase in the burnishing force and with a decrease in the feed. The comparison of various methods of analysis of positron annihilation lifetime (PAL) spectra allowed identification of two components, which are related to solute-vacancy complexes and vacancy clusters, respectively. It was found that the increase in microhardness was related to the increase in the concentration of vacancy clusters.

Key words: AZ91HP magnesium alloy • defects • positron lifetime annihilation spectroscopy (PALS) • roller burnishing • Vickers' hardness test

Introduction

Magnesium alloys are very lightweight materials. The density of Mg alloys is only 65% of the density of commonly used aluminum alloys. Thus, replacement of aluminum alloys by magnesium ones allows weight reduction without compromising overall strength. Moreover, Mg alloys are an alternative to some engineering plastics due to their higher stiffness and recycling capabilities. These features make Mg alloys promising engineering materials for automotive and aerospace industries.

The fatigue performance of load-bearing Mg parts has to be improved to fulfill the high requirements of the industry for mechanical properties. This goal is usually achieved by shot peening or roller burnishing the surface of the parts. It was found that the latter method results in a greater increase in the fatigue strength [1, 2]. Roller burnishing is a manufacturing process used to improve surface roughness, increase hardness of the surface layer, and introduce compressive residual stresses. Mg alloys are classified into cast and wrought alloys. Most previous investigations of roller burnishing of Mg alloys were carried out on wrought alloys [2–4], thus it seems interesting to extend studies to cast alloys, e.g. AZ91HP.

The objective of the current study is to determine the effect of roller burnishing on the defect structure in AZ91HP Mg alloy. The standard Vickers' method was supplemented by positron annihilation lifetime

R. Zaleski✉, M. Gorgol
Department of Nuclear Methods,
Institute of Physics,
Maria Curie-Skłodowska University,
1 M. Curie-Skłodowskiej Sq., 20-031 Lublin, Poland,
Tel.: +48 81 537 6145, Fax: +48 81 537 6191,
E-mail: radek@zaleski.umcs.pl

K. Zaleski
Faculty of Mechanical Engineering,
Lublin University of Technology,
36 Nadbystrzycka Str., 20-618 Lublin, Poland

Received: 26 June 2015
Accepted: 27 August 2015

Table 1. Chemical composition of the AZ91HP Mg alloy

Element	Mg	Al	Zn	Si	Ni	Mn	Cu	Fe
Mass fraction [%]	Balance	9.45	0.72	0.03	0.025	0.017	0.016	0.002

spectroscopy (PALS) to obtain complementary data. The possibility of studying effects of burnishing in the surface layer of steel and titanium alloys using this method has already been tested [5, 6]. In this work, we will evaluate PALS capability to investigate structure changes caused by roller burnishing of an Mg alloy.

Materials

The AZ91HP alloy is a cast Mg alloy characterized by great purity and corrosion resistance. This alloy is used mainly in the aircraft, automotive, and electrical industry. Bar-shaped samples with dimensions 4 mm × 15 mm × 100 mm made of the AZ91HP Mg alloy were used. The AZ91HP alloy composition is presented in Table 1.

The surface of the samples was milled before burnishing. No heat treatment was applied to keep the conditions used in the industry. Then the samples were fixed on the frontal area of a dedicated lathe chuck. They were burnished on a lathe roller using a burnisher ball. The diameter of the burnisher ball $D = 16$ mm and burnishing speed $v = 56$ m/min were constant for all samples. The variable parameter of burnishing was force F , which was changed between 150 N and 750 N at the constant feed $f = 0.14$ mm/rev. Alternatively, the feed f was changed within a range of 0.05–0.62 mm/rev. at the constant burnishing force $F = 450$ N.

Experimental

Microhardness measurements were made using a LECO's LM700AT microhardness tester. The burnished surface of the samples was tested using the Vickers' method with the load of 0.981 N.

The PALS measurements were conducted using a standard fast-slow delayed coincidence spectrom-

eter. The ^{22}Na positron source inside a Kapton envelope was placed between two bars of the Mg alloy, which were subjected to the same treatment. Such a sandwich-shaped sample was placed between two scintillation detectors equipped with BaF_2 scintillators. The resolution curve was approximated by a single Gaussian with average FWHM = 240.4(4) ps. Positron annihilation lifetime spectra were collected for 24 hours for each sample, which guaranteed that the total count number reached 10^7 .

PAL spectra analyses were performed using the LT program [7]. The contribution of positrons annihilating inside the Kapton envelope with a lifetime of 374 ps was fixed at 12%. This is in good agreement with Ref. [8], where the fraction of annihilation in Kapton was found to be 12% in Kapton foil with the same thickness between Mg samples as well as with Monte Carlo simulation [9], which gives 11.7%.

Results and discussion

The results of microhardness measurement (Fig. 1) show a great impact of ball burnishing on the hardening of the surface layer. Its microhardness increases by 40% at both the greatest burnishing force (F) and the greatest inverse of feed ($1/f$) (i.e., density of burnishing tool passes). However, the dependences of microhardness on these parameters are different. The dependence on F is almost linear, thus its further increase could give even greater hardening. In turn, it seems that a further increase of $1/f$ would not result in a significant increase in microhardness, because at 20 rev./mm it almost reached its saturation.

A single positron component with a lifetime of 219.7(4) ps was found in the non-burnished sample of the AZ91HP Mg alloy. A single component spectrum is often observed in untreated Mg-rich alloys, but usually its lifetime is closer to 225 ps [8, 10–13]. However, a lifetime of 220 ps was also reported [14]. There are two ways of explaining the lack of

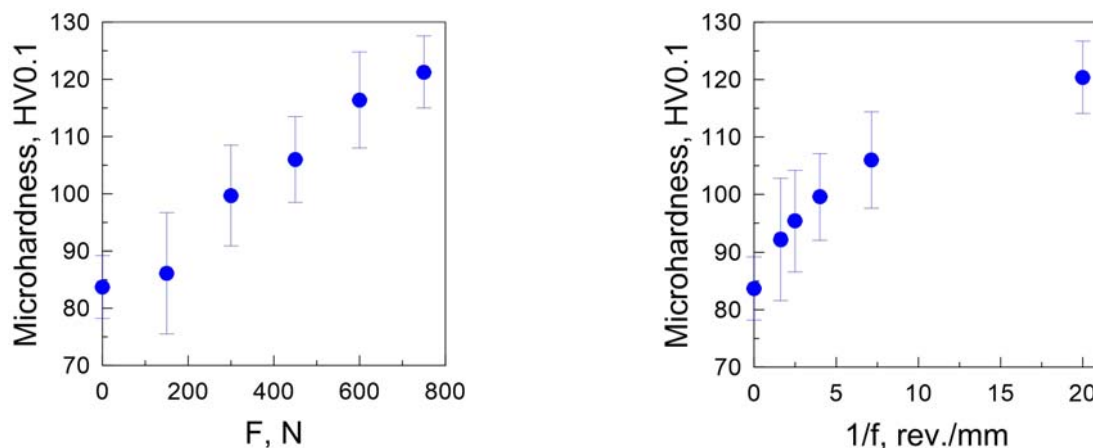


Fig. 1. Microhardness of the AZ91HP Mg alloy as a function of the burnishing force at $1/f = 7.1$ rev./mm (left) and the inverse of feed at $F = 450$ N (right).

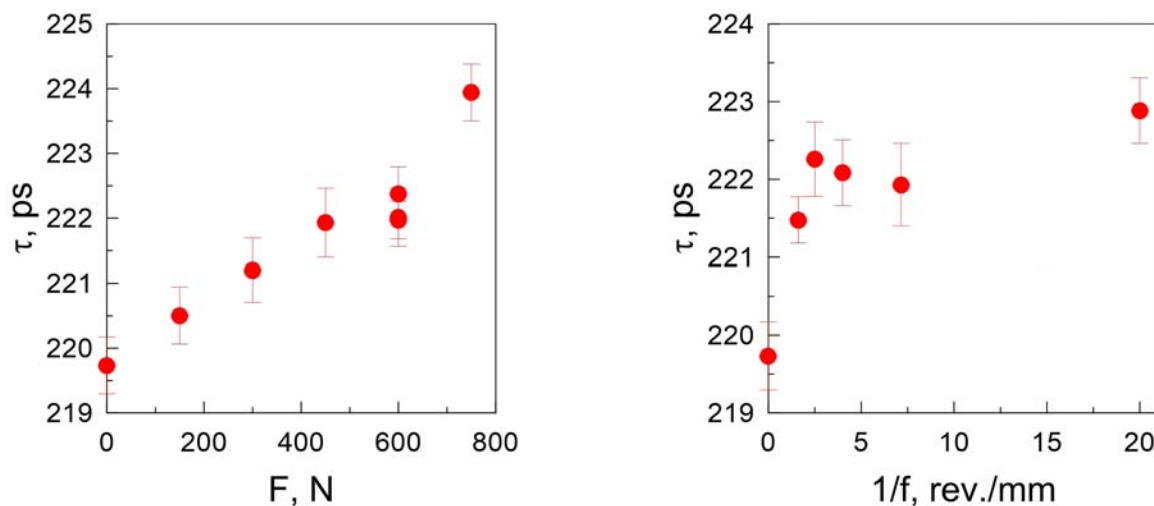


Fig. 2. Lifetime of positrons obtained by single component fitting in the AZ91HP Mg alloy as a function of the burishing force at $1/f = 7.1$ rev./mm (left) and the inverse of feed at $F = 450$ N (right).

other components: either all positrons annihilate in bulk Mg because the concentration of open-volume defects is lower than the PALS detection threshold (10^{-6}) [11] or, in contrast, all positrons are trapped in defects. The lifetime expected for the Mg bulk value was found to be between 218 ps and 225 ps [10, 15–18]. Thus, the lifetime observed in the AZ91HP alloy would rather point to the first explanation. However, the comparison between positron lifetimes and Doppler broadening study [8, 14] shows that the same lifetimes are observed for positrons trapped in vacancies in a solute-rich environment (i.e., most likely, Al-vacancy or Zn-vacancy complexes in AZ91HP). Because the origin of this component cannot be determined based on its lifetime, it will be discussed based on two different methods of spectra analysis in the later part of the article.

Our intention is to compare the PALS results with microhardness. Unfortunately, the changes of PAL spectra are much smaller than those of microhardness. Approximating the spectra for all samples by a single component shows that the difference between their lifetimes is at most 2% (Fig. 2). The repeatability of the results was verified by the comparison of three subsequent measurements for $F = 600$ N, also presented in Fig. 2. The fairly good fit ($\chi^2 = 1.03$ – 1.34) indicates that the contribution of any other component is small, if it is present at all. The lifetime follows the changes in the microhardness, when F is changed at the constant feed. In turn, it reaches saturation much faster than the microhardness for the dependence against $1/f$.

The interpretation of the PAL spectra in terms of the microstructure requires quantitative results of a possibly accurate reconstruction of their components. This task is difficult due to the very subtle differences between the spectra. If we assume that before burishing only the bulk lifetime (τ_b) was present and, a component originating from defects appears after it, the use of the two-state simple trapping model (STM) [19] is appropriate. According to the STM, τ_b is given by

$$(1) \quad \frac{1}{\tau_b} = \frac{I_1}{\tau_1} + \frac{I_2}{\tau_2}$$

that is, a combination of the intensities (I_i) and lifetimes (τ_i) of two components ($i = 1, 2$) present in a spectrum. Additionally, the positron-trapping rate in defects (κ) is given by

$$(2) \quad \kappa = \frac{I_2}{I_1} \left(\frac{1}{\tau_b} - \frac{1}{\tau_2} \right).$$

A scatter that blurs the results could be avoided only if the lifetimes in a bulk and defects were assumed as the fitting parameters, whose values are common for all spectra. The lifetime $\tau_b = 220.0(1)$ ps obtained in this way is consistent with the lifetime observed in the non-burnished sample. The lifetime in defects $\tau_2 = 281(7)$ ps is intermediate between lifetimes characteristic for dislocation (~ 255 ps) and monovacancy (~ 300 ps) in Mg [15, 17, 18]. This suggests that both these defects exist in the samples. This also proves that assuming the common value of this lifetime in all samples is only a rough approximation, because it is hardly possible that the ratio between these two defects is the same in every sample. The intensity of the component related to defects and the positron trapping rate follow the same tendency as the lifetime in the single component analysis (Fig. 3). This confirms that the changes in the lifetime in the single component analysis are in fact caused by the varying contribution of the second component. The fit obtained using STM ($\chi^2 = 1.04$ – 1.29) is practically the same as in the single component analysis. Thus, STM analysis does not provide a significantly more accurate reconstruction of the spectra.

Another approach to the analysis of the spectra is fitting two components regardless of the STM. Rejection of the constraints imposed by the STM resulted in finding a very similar lifetime (τ_1) of the short-lived component for all spectra and reduction of the scatter of the results. The average value of this lifetime $\langle \tau_1 \rangle = 220(1)$ ps is again consistent with the result of the single component analysis. In contrast, the lifetime of the long-lived component (τ_2) differs significantly among the spectra. It is clearly longer ($\langle \tau_2 \rangle = 471(111)$ ps) than the one obtained from the STM analysis. A further decrease in the scatter was achieved by fixing τ_1 at its average value. It did not cause any deterioration of the fit, which was

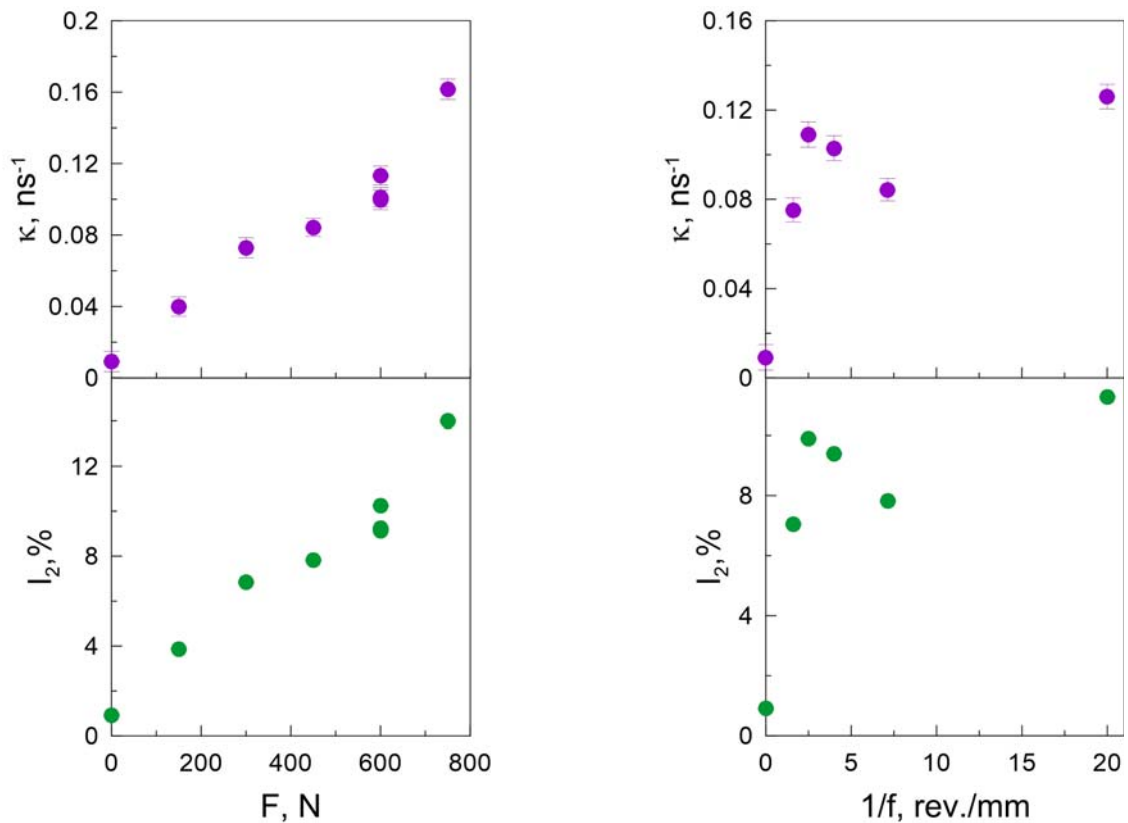


Fig. 3. Positron trapping rate and intensity of the component related to defects obtained by fitting STM in the AZ91HP Mg alloy as a function of the burnishing force at $1/f = 7.1$ rev/mm (left) and the inverse of feed at $F = 450$ N (right).

clearly better compared to the previous analysis ($\chi^2 = 0.96\text{--}1.10$). The lifetime τ_2 decreases with an increase in F and $1/f$ (Fig. 4), but it is difficult to interpret

until it falls below ca. 440 ps, which is a saturation lifetime for very large clusters of vacancies in Mg [17, 18]. Therefore, τ_2 is most likely overestimated

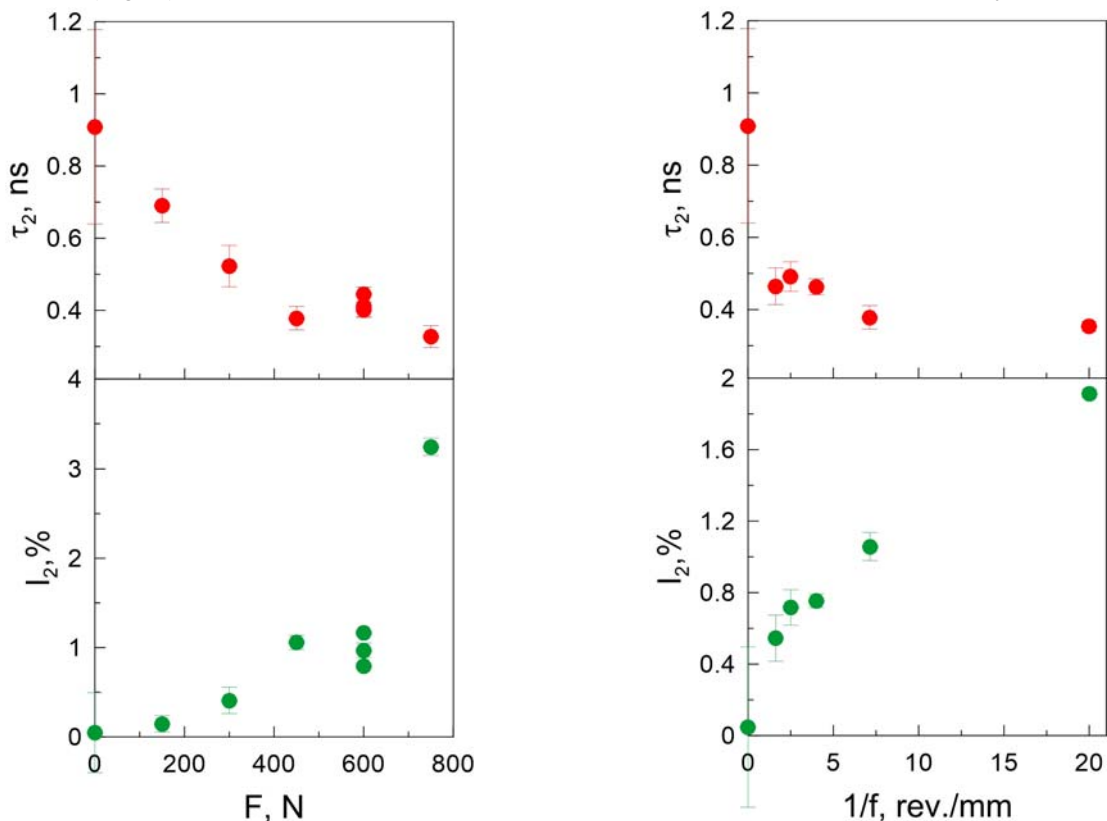


Fig. 4. Lifetime and intensity of the long-lived component obtained by two component fitting in the AZ91HP Mg alloy as a function of the burnishing force at $1/f = 7.1$ rev/mm (left) and the inverse of feed at $F = 450$ N (right).

due to too low I_2 if it is below 0.5%. Alternatively, this component can be a mixture of the lifetime in vacancy clusters and a long-lived o -Ps lifetime in the positron source (NaCl). In such a case, the observed component is an average lifetime. Even very small contribution ($\sim 0.1\%$) from the source predominates if the concentration of the vacancy clusters is low. For the same reasons, the result for the non-burnished sample confirms only that no component related to defects is present in this sample and should not be taken into account. For intensities above 1%, τ_2 stabilizes at ca. 350 ps, which corresponds to four vacancy clusters. Still, we cannot reject that large vacancies are formed at small F and $1/f$. The intensities I_2 are much lower than in the STM analysis. Their dependencies vs. F and $1/f$ are most similar to dependencies of microhardness among all the presented.

Conclusions

The poor susceptibility of PAL spectra to the changes in the magnesium alloy caused by ball burnishing makes analysis of the data and interpretation of the results challenging. Among the three presented methods of analysis, the two-component analysis seems to give the most reliable results. They are most consistent with the results of macroscopic Vickers' method. Although the lifetimes for F smaller than 400 N are overestimated, the rest of the results allow determination of most likely changes in the microstructure of the AZ91HP Mg alloy. A small number of large clusters of vacancies are formed when the feed is large or the burnishing force is small. The clusters become smaller (i.e., they contain several vacancies) and their concentration grows if the force increases or the feed decreases. The short-lived component can hardly be attributed to positron annihilation in bulk material, because in such a case its lifetime would not be constant among the samples, as shown by the STM. Thus, it is most likely that this component is in fact annihilation of the positrons trapped in a solute-vacancy complex. In such a case, no positron transfer from this state to another one would be present. Instead, there would be only competition between positron trapping in the solute-vacancy complexes and the vacancy clusters.

Acknowledgment. Financial support of Structural Funds in the Operational Programme-Innovative Economy (IEOP) financed from the European Regional Development Fund – Project “Modern material technologies in aerospace industry”, POIG.01.01.02-00-015/08-00 is gratefully acknowledged.

References

1. Zhang, P., & Lindemann, J. (2005). Influence of shot peening on high cycle fatigue properties of the high-strength wrought magnesium alloy AZ80. *Scripta Mater.*, 52(6), 485–490. DOI: 10.1016/j.scriptamat.2004.11.003.

2. Zhang, P., & Lindemann, J. (2005). Effect of roller burnishing on the high cycle fatigue performance of the high-strength wrought magnesium alloy AZ80. *Scripta Mater.*, 52(10), 1011–1015. DOI: 10.1016/j.scriptamat.2005.01.026.
3. Fouad, Y. (2011). Fatigue behavior of a rolled AZ31 magnesium alloy after surface treatment by EP and BB conditions. *Alexandria Eng. J.*, 50(1), 23–27. DOI: 10.1016/j.aej.2011.01.004.
4. Pu, Z., Yang, S., Song, G. L., Dillon Jr, O. W., Puleo, D. A., & Jawahir, I. S. (2011). Ultrafine-grained surface layer on Mg-Al-Zn alloy produced by cryogenic burnishing for enhanced corrosion resistance. *Scripta Mater.*, 65(6), 520–523. DOI: 10.1016/j.scriptamat.2011.06.015.
5. Zaleski, R., & Zaleski, K. (2006). Positron annihilation in steel burnished by vibratory shot peening. *Acta Phys. Pol. A*, 110(5), 739–746.
6. Zaleski, K., & Zaleski, R. (2009). Badania warstwy wierzchniej stopu tytanu technikami wykorzystującymi anihilację pozytonów. *Inżynieria Materiałowa*, 5, 302–305.
7. Kansy, J. (1996). Microcomputer program for analysis of positron annihilation lifetime spectra. *Nucl. Instrum. Methods Phys. Res. Sect. A-Accel. Spectrom. Dect. Assoc. Equip.*, 374(2), 235–244. DOI: 10.1016/0168-9002(96)00075-7.
8. Mengucci, P., Barucca, G., Riontino, G., Lussana, D., Massazza, M., Ferragut, R., & Aly, E. H. (2008). Structure evolution of a WE43 Mg alloy submitted to different thermal treatments. *Mater. Sci. Eng. A*, 479(1/2), 37–44. DOI: 10.1016/j.msea.2007.06.016.
9. Djourelou, N., & Misheva, M. (1996). Source correction in positron annihilation lifetime spectroscopy. *J. Phys.-Condens. Mat.*, 8(12), 2081. DOI: 10.1088/0953-8984/8/12/020.
10. Čížek, J., Procházka, I., Smola, B., Stulíková, I., & Očenášek, V. (2007). Influence of deformation on precipitation process in Mg-15 wt.%Gd alloy. *J. Alloys Compd.*, 430(1/2), 92–96. DOI: 10.1016/j.jallcom.2006.03.097.
11. Čížek, J., Vlček, M., Smola, B., Stulíková, I., Procházka, I., Kužel, R., Jäger, A., & Lejček, P. (2012). Vacancy-like defects associated with icosahedral phase in Mg-Y-Nd-Zr alloys modified by the addition of Zn. *Scripta Mater.*, 66(9), 630–633. DOI: 10.1016/j.scriptamat.2012.01.054.
12. Dryzek, J., & Dryzek, E. (2007). The subsurface zone in magnesium alloy studied by positron annihilation techniques. *Tribol. Int.*, 40(9), 1360–1368. DOI: 10.1016/j.triboint.2007.03.004.
13. Ortega, Y., & Rio, Jd. (2005). Study of Mg-Ca alloys by positron annihilation technique. *Scripta Mater.*, 52(3), 181–186. DOI: 10.1016/j.scriptamat.2004.09.033.
14. Moia, F., Calloni, A., Ferragut, R., Dupasquier, A., Macchi, C. E., Somoza, A., & Jian Feng Nie (2009). Vacancy-solute interaction in magnesium alloy WE54 during artificial ageing: a positron annihilation spectroscopy study. *Int. J. Mater. Res.*, 100(3), 378–381. DOI: 10.3139/146.110036.
15. Čížek, J., Procházka, I., Smola, B., Stulíková, I., Kužel, R., Matěj, Z., & Cherkaska, V. (2006). Thermal development of microstructure and precipitation effects in Mg-10wt%Gd alloy. *Phys. Status Solidi A*, 203(3), 466–477. DOI: 10.1002/pssa.200521483.
16. Hautojärvi, P., Johansson, J., Vehanen, A., Yli-Kaupilla, J., Hillairet, J., & Tzanétakis, P. (1982). Trapping of positrons at vacancies in magnesium. *Appl. Phys. A*, 27(1), 49–56. DOI: 10.1007/BF01197546.

17. Checchetto, R., Bazzanella, N., Kale, A., Miotello, A., Mariazzi, S., Brusa, R. S., Mengucci, P., Macchi, C., Somoza, A., Egger, W., & Ravelli, L. (2011). Enhanced kinetics of hydride-metal phase transition in magnesium by vacancy clustering. *Phys. Rev. B*, 84(5), 054115. DOI: 10.1103/PhysRevB.84.054115.
18. Luna, C. R., Macchi, C., Juan, A., & Somoza, A. (2013). Vacancy clustering in pure metals: some first principle calculations of positron lifetimes and momentum distributions. *J. Phys. Conf. Ser.*, 443(1), 012019. DOI: 10.1088/1742-6596/443/1/012019.
19. Brandt, W. (1974). Positron dynamics in solids. *Appl. Phys.*, 5(1), 1–23. DOI: 10.1007/BF01193389.